



Full Text View

[Volume 32, Issue 5 \(May 2002\)](#)

Journal of Physical Oceanography

Article: pp. 1585–1592 | [Abstract](#) | [PDF \(1.61M\)](#)

SST Observations of the Agulhas and East Madagascar Retroflexions by the TRMM Microwave Imager

Graham D. Quartly and Meric A. Srokosz

James Rennell Division for Ocean Circulation and Climate, Southampton Oceanography Centre, Southampton, United Kingdom

(Manuscript received September 28, 2000, in final form November 13, 2001)

DOI: 10.1175/1520-0485(2002)032<1585:SOOTAA>2.0.CO;2

ABSTRACT

The retroflexions of the East Madagascar Current and Agulhas Current are complex rapidly evolving systems, the latter controlling the passage of warm salty water from the Indian Ocean to the Atlantic. The TRMM Microwave Imager (TMI) provides frequent observations of sea surface temperature through clouds, allowing one to monitor the evolution of these systems. The authors develop a simple feature-tracking system that obviates the need for user intervention, and use its results to guide more focused studies. In the period 1997–99, westward progradation of the Agulhas retroflexion (associated with ring shedding) is observed about eight times per year, agreeing with previous estimates from infrared data, and many rings move westward or northwestward. However, this behavior is seen to change in the 2000–01 time period, with the Agulhas retroflexion occurring farther to the east. A few Natal pulses are seen, but cannot be linked conclusively to the spawning of rings due to TMI's limited latitudinal coverage. The majority of features originating at the East Madagascar retroflexion appear to migrate southwestward. A new observation from the data is that, although the first northward meander of the Agulhas Return Current is constrained by bathymetry, its position does vary intermittently, remaining fixed in a given location for up to six months at a time. Southward propagation of features is noted along two ridges: although eddies have been found before along the eastern slope of the Mozambique Ridge, the new results for the Madagascar Ridge indicate an extra pathway for the eddies. Eddylike features are also found leading from the Agulhas Return Current back toward the Agulhas Current. The narrow “corridor” of these features suggests that it is controlled by the gyre recirculation in the southwest Indian Ocean.

Table of Contents:

- [Introduction](#)
- [TRMM Microwave Imager](#)
- [Feature tracking: Method](#)
- [Hovmöller analysis:](#)
- [Conclusions](#)
- [REFERENCES](#)
- [FIGURES](#)

Options:

- [Create Reference](#)
- [Email this Article](#)
- [Add to MyArchive](#)
- [Search AMS Glossary](#)

Search CrossRef for:

- [Articles Citing This Article](#)

Search Google Scholar for:

- [Graham D. Quartly](#)
- [Meric A. Srokosz](#)

The Agulhas Current (AC) is the strongest Southern Hemisphere western boundary current, with a narrow well-defined thermal signature along the east coast of South Africa. On leaving the coast at $\sim 25^\circ\text{E}$, conservation of potential vorticity causes it to retroflect $\sim 500\text{--}600$ km farther south, forming the eastward-flowing Agulhas Return Current (ARC), which has significant meanders, partly constrained by the local bathymetry (see [Fig. 1](#)). This is an eddy-rich region with Agulhas rings ~ 200 km in diameter being shed at the retroflection and large eddies occurring along the ARC ([Olson and Evans 1986](#); [Gründlingh 1983](#); [Lutjeharms and Valentine 1988](#)). The AC is fed by the Mozambique Current and the East Madagascar Current (EMC), but there is debate about their relative contributions ([de Ruijter et al. 1999a](#)). Indeed, recent in situ observations by [de Ruijter et al. \(2001\)](#) suggest that the Mozambique Current is not itself a permanent feature, but only present intermittently as anticyclonic eddies pass through the Mozambique Channel. [Lutjeharms \(1988a\)](#) shows that south of Madagascar the EMC also exhibits a retroflection. Feed from the EMC to the AC may thus be via a thin remnant adhering to the south coast of Madagascar or by westward movement of eddies shed from this retroflection. Drifter data has shown that the latter may be the case at least some of the time ([Lutjeharms 1988b](#)). Here we look at the new insights that can be gained from TRMM Microwave Imager (TMI) data to aid our understanding of both retroflection systems. [Section 2](#) describes the data and processing; [section 3](#) explains the simple feature-tracking technique and its results, with a more focussed regional analysis given in [section 4](#). We end with a brief discussion and conclusions.

2. TRMM Microwave Imager (TMI): Data and processing

The TMI is a multichannel scanning passive microwave radiometer, designed for observing precipitation. However, its 10.7-GHz channel permits the recovery, through nonraining clouds, of sea surface temperature (SST) data. These have been shown to agree well with buoy measurements ([Wentz et al. 2000](#)). TRMM's low altitude (350 km) gives an antenna footprint at 10.7 GHz of $35\text{ km} \times 60\text{ km}$ ([Kummerow et al. 1998](#)), suitable for detecting mesoscale features. However, SST values close to the coast will be contaminated by the influence of land. We have used daily files of SST gridded at 0.25° by 0.25° , which are provided by the Earth Observation Research Center (EORC)/National Space Development Agency (NASDA) (<http://www.eorc.nasda.go.jp/TRMM>).

The inclination of the TRMM orbit is 35° , so the TMI data only extend as far south as 38°S , just short of the main region of the Agulhas retroflection (AR) and mean ARC. The rest of the area of interest ([Fig. 1](#)) is observed at least once every day. Because of the satellite's low altitude, the TMI swath does not cover all regions within one day. To minimize errors, especially biases associated with variation in day/night sampling, we composite the data in 6-day averages, as large features will not change greatly in such a period. We form the 6-day averages at intervals of 3 days to make it easier to monitor changes in the spatial arrangements. We then apply a smoothing filter (~ 100 km in diameter) to remove finer scale structure, yet leave the signature of the AC and associated eddy features undiminished. Data from 8 December 1997 to 31 July 2001 provide us with 443 composite SST maps, 3 days apart. We apply EOF analysis to characterize and remove the large-scale coherent variations in SST. For example, the first two modes of variation are the mean and seasonal signals. The third and fourth modes principally represent meridional changes in SST to the west of South Africa, with the fourth mode probably portraying changes in upwelling, in response to changes in winds. Here, we remove the first five EOF modes from the data to make the motion of the smaller scale features clearer. Experiments removing different numbers (3, 4, 5) of EOFs changes the picture obtained in terms of the fine detail, but do not impact the overall results presented below. [Figure 2](#) illustrates the result of this initial filtering of the data. The top image shows the original SST field for the period 23–28 January 1999, and the middle one shows the result of filtering, which removes the mean AC and the Benguela upwelling. Eddylike features abound, including a region of enhanced temperature on the edge of the AC (marked by a box). [Figure 2c](#) shows the rms variability of the filtered SST data, with high variability along the coast of South Africa and Madagascar, and also along the southern and eastern boundaries of the region. There are large areas for which the residual variability is less than 0.4°C ; these indicate regions for which there is little SST variation that is not adequately represented by the first five EOFs. To get a clearer picture of the variations we apply simple feature-tracking and then (in [section 4](#)) examine Hovmöller diagrams for selected regions.

3. Feature tracking: Method and results

The filtering produces SST anomalies; clearly nonchanging features will have no signal. To track features we find local maxima in the filtered SST field and, using a search box ~ 200 km square centered on a maximum, examine the immediately preceding and succeeding fields. If a “significant” feature is found then tracking is continued a further step, using a box centered on the new location. The tracking ends if either the peak falls below 0.4°C or it is located on the edge of the box (possibly indicating that tracking has jumped to a larger feature centered outside the box). This is a simple scheme to determine the main propagation directions of features, and so makes no assumption that features will continue to move in the same direction. [Olson and Evans \(1986\)](#) and [Goni et al. \(1997\)](#) noted that Agulhas rings often show sharp changes in trajectory early on in their life. As the feature-tracking is quite simplistic, many of the tracks are short, possibly due to features being “lost” for a while when their surface signature becomes small. Thus the feature tracking is only indicative of the direction of motion of the stronger SST anomalies, rather than giving a complete time history of all events. However, a series of trials with slightly different SST thresholds or tracking strategies produced the same basic results detailed here.

The analysis was performed for both positive anomalies (SST anomaly $\geq 0.4^\circ\text{C}$) and negative ones (SST anomaly \leq

-0.4°C) and the 250 largest amplitude events of each type are shown in [Fig. 3](#). Although many of the tracks are short, the ensemble provides a coherent picture. The tracking for negative anomalies is shown so as both to highlight any features with a negative signature and also to act as a contrast to [Fig. 3a](#). Since we are looking at anomalies, a series of cold core eddies (negative anomalies) along a path may lead to the appearance of positive anomalies along that route (effectively due to the gaps between the eddies). It is thus interesting that the negative anomalies do not show the same coherent patterns.

The positive anomalies indicate significant activity to the south of Madagascar. Most of the features head southward along the Madagascar Ridge and then southwestwards. The track of the positive anomalies ties in with the enhanced SST variability in [Fig. 2c](#). As this is not known to be the route of the EMC after retroflection, it seems likely that these are eddies shed at the retroflection. It was surprising that none appear to make the direct westward progression to the AC as expected from drifter tracks ([Lutjeharms 1988b](#)) and high-resolution models ([Bjastoch and Krauss 1999](#)); their apparent absence may be due to such a path being approximately along an isotherm (see [Fig. 2a](#)). Thus such propagating features would produce little by way of SST anomaly.

A large number of features head poleward along the east coast of South Africa. There are few positive features on the mean axis of the AC; rather most move down the seaward side, where an advected eddy or a large-scale meander of the current can lead to a large positive SST anomaly. This is especially true after leaving the coast, where the mean AC is marked by a strip free of warm anomalies. It is likely that some of these positive anomalies are Natal pulses, large offshore meanders of the AC. These are intermittent features, extending more than 200 km from the shore ([Gründlingh 1979](#)) and propagating along the coast at approximately 20 km day^{-1} ([Lutjeharms and Roberts 1988](#); [van Leeuwen et al. 2000](#)).

The region to the southwest of South Africa is where one would expect to find recently spawned Agulhas rings. These usually consist of a pinched off segment of warm water from the AC plus colder entrained water. Should these features move northward, their cores will be colder than the surrounding region, giving rise to negative anomalies. Agulhas rings may thus be detected as both positive (warm) and negative (cold) anomalies: both [Figs. 3a and 3b](#) show westward or northwestward movement in this region. Long trajectories should not be expected for either type of feature since it is known that once separated from the AC, ocean-atmosphere heat fluxes will rapidly erode the surface thermal signature ([Walker and Mey 1988](#)).


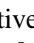

There are a number of features moving roughly southward around 35.5°E, which marks the eastern edge of the Mozambique Ridge (see [Fig. 1](#)). It is conjectured that these may be cyclonic eddies that are deep enough to be steered by the bathymetry. Although such features have a “cold core” with lifting of all isotherms below 300 m ([Gründlingh 1983, 1985](#)) they usually have a positive SST anomaly. On the right-hand side of [Fig. 3b](#) a number of negative anomalies can be seen moving northwestward from 36°S, 48°E.

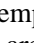
As noted above, the analysis was repeated with broader smoothing, and also with different numbers of EOFs removed. Although the tracking of individual features was affected, the overall pattern remained the same. A few of the key regions are examined in greater detail in the next section.

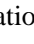
4. Hovmöller analysis: Regional studies

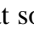
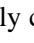
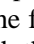
Having identified some of the main paths, we examine the time evolution using Hovmöller plots. [Figure 4a](#) shows the progression of spatially averaged anomalies for the band 34.5°–36.5°E. (Note, these are longitudinal averages of anomalies about a temporal mean.) This is a region of above average variability (see [Fig. 2c](#)) and appears to be a preferred route for positive anomalies (see [Fig. 3a](#)). From 25° to 30°S this corresponds to the region just offshore of the AC, while farther south it represents the eastern flank of the Mozambique Ridge. During the 44-month period there are indications of seven positive anomaly features propagating along this meridional section, albeit that the signals in the later part of the observation period (March 2000 onward) are less distinct than their predecessors. (Although alignments are seen in negative anomalies they are rarely as clear as the positive ones.) In several cases two straight lines are needed to indicate one trajectory, with the “break point” being near 500 km, which corresponds to a latitude of 34°S. For events 1, 2, 4, 5, and 6 the estimated propagation speeds north of 34°S have a mean of 12.1 km day^{-1} (std dev = 2.6 km day^{-1}). For events 1, 2, 3, 5, 6, and 7 there is a phase of slower propagation (mean = 3.8 km day^{-1} , std dev = 0.7 km day^{-1}) in the southern region of the section. These slower speeds are similar to the eddy advection velocities of 4–5 km day^{-1} noted in this region by [Gründlingh \(1983, 1985\)](#).

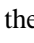
To monitor features following the coast, we calculate the mean SST anomaly for each point along the coast using a ~200 km transect on a bearing of 120° (see [Fig. 2c](#)). The resultant features ([Fig. 4b](#)) are intermittent and show significant changes in propagation speed. A number of coherent poleward moving features can be seen, highlighted by dashed lines. The lines for Event E (February 1999) were chosen to indicate a velocity of 20 km day^{-1} for the first 900 km (the approximate distance from the Natal Bight to a little south of Port Elizabeth, where the AC leaves the coastal confines for deeper waters) and 5 km day^{-1} subsequently. These are values from analysis of infrared data ([van Leeuwen et al. 2000](#)),

and confirm that some of the features in [Fig. 4b](#)  have propagation characteristics consistent with those observed for Natal pulses. Up to seven poleward-moving positive anomaly features can be seen in [Fig. 4b](#)  in the period up to May 1999. All give rise to a temperature anomaly of $\sim 0.6^\circ\text{C}$ when averaged over a 200-km transect, and maintain this amplitude for most of their 1000-km journey beyond the Natal Bight. A number seem to originate from much further up the coast. This suggests that these meanders started farther north in the Delagoa Bight, although these earlier signals could be migrating eddies which initiate a meander only on reaching the shallow shelf of the Natal Bight ([de Ruijter et al. 1999b](#)). The signals are not so coherent after May 1999. Two further propagating features are marked, but they are weaker than their predecessors and do not travel to the end of the specified path. Using TOPEX/Poseidon altimeter data, we made a brief examination of the sea surface height (SSH) averaged near 29°E , 32°S . The small circles at the 400 km mark in [Fig. 4b](#)  indicate times when the SSH was significantly lower at that location compared to elsewhere in that region. [Van Leeuwen et al. \(2000\)](#) have shown that a Natal Pulse should lead to a local reduction in SSH. Of the ten SSH features marked, six lie close to the lines deduced from TMI SST data, and two others correspond to positive SST anomalies that are not propagating.

The dashed lines on [Fig. 4b](#)  are mainly to emphasize the features, with the slopes of the lines corresponding to propagation speeds. Clearly some of the features are not represented well by a single straight line. For the coastal section between 0 and 900 km from the Natal Bight, the derived propagation speeds range between 13 and 55 km day^{-1} . The maximum value (from case G) is much higher than reported elsewhere, and is probably a result of attempting to match it to the positive anomalies north of the Natal Bight. The median of the nine measurements is 25 km day^{-1} , which is close to the value of 20 km day^{-1} noted by [Lutjeharms and Roberts \(1988\)](#). [Lutjeharms et al. \(2001\)](#) have suggested that by $26^\circ\text{--}28^\circ\text{E}$ the speed of Natal pulses may be as slow as 11 km day^{-1} . [Lutjeharms and Roberts \(1988\)](#) also note that the speed reduces to around 5 km day^{-1} upon leaving the coast at Port Elizabeth (approximately 900 km from the Natal Bight). We have noted that features A, B, and E do show a slower speed after there, but it is hard to estimate the values over such a relatively short extent.

The southern limit of TMI's coverage means it is impossible to observe ring shedding from the Agulhas retroflection directly. The best we can do is monitor the western edge of the AC as it disappears from the frame of view. We take the original smoothed dataset including the mean signal, and calculate the zonal gradient at 38°S to highlight the sharp change. [Figure 4c](#)  shows repeated westward progradation, with 17 possible events in the first two years. If all are separate events, this gives an average close to the 9 yr^{-1} found by [Lutjeharms and van Ballegooyen \(1988\)](#) from infrared data. However, some "events" are not completely distinct from their neighbors in time; a lower bound on the number of events is 6 yr^{-1} , a value [Feron et al. \(1992\)](#) found from altimetry. The disparity between estimates *may* be due to anomalous or partial westward progradation of the AR, but with the release of an eddy to the south, which is subsequently advected east rather than transporting Indian Ocean water into the Atlantic. No clear progradation is observed during February to September 2000; [van Leeuwen et al. \(2000\)](#) noted a 6-month period of inactivity in late 1993. Thereafter there appears to be one clear event followed again by another 6-month "quiet" period until the end of April 2001. The mean progradation rate observed in the TMI data is $11.9 \pm 2.3 \text{ km day}^{-1}$, agreeing with [Lutjeharms and van Ballegooyen's \(1988\)](#) 12 km day^{-1} .

The observations ([Fig. 4](#) ) clearly show that something unusual occurred during 2000–01. Features along all three of these sections either disappeared or had a much weaker signature. Toward the end of 2000 there is a significant change in the behavior of the AC system. This is not entirely clear in the data shown in [Fig. 4](#) , but by examining an animation of TMI SST pictures we have found that during the period October 2000–March 2001 the Agulhas Current appears to leave the coast in a more southerly direction. As a result the feature seen in [Fig. 4c](#)  at $\sim 26^\circ\text{E}$ propagating toward $\sim 20^\circ\text{E}$, during December 2000 to March 2001, is associated with the AC rather than with the meander in the ARC as is the case earlier in the observations. It is unclear what has caused this change in the circulation of the AC system. It is known that, if the AC is stronger, it will tend to leave the coast in a more southerly direction, while, if it is weaker, it will tend to follow the topography in a more southwesterly direction (see discussion in [Quarty and Srokosz 1993](#) and references therein).

The changed location of the AC during late 2000 may explain why the possible Natal pulse feature H appears to die out; the main axis of the current directs it away from the specified section used in this Hovmöller analysis ([Fig. 2c](#) ). The TMI analysis does not reveal a clear correspondence between Natal pulses and ring shedding as noted by [van Leeuwen et al. \(2000\)](#), using altimeter and infrared observations. However, it is possible that feature H helps instigate the return of the AC to its normal path.

We observed no clear Natal pulse during June 1999 to June 2000, and only one clear progradation of the Agulhas Retroflection during January 2000 to April 2001. [Van Leeuwen et al. \(2000\)](#) commented on an absence of Natal pulses in the second half of 1993, and [Schouten et al \(2000\)](#) found only one clear ring-shedding event during each of September 1993 to March 1994 and August 1995 to April 1996. These observations are suggestive of the idea that El Niño activity may have a delayed effect on the Agulhas Current region ([Schouten et al. 2001](#), manuscript submitted to *Geophys. Res. Lett.*); the effects observed here being linked in some way to the 1997/98 event.

Near 26°E there is a sharp change between negative and positive gradients, representing the centre of a meander in the

ARC. This feature is emphasized by the dotted lines, and the observations indicate that it is not completely fixed, despite the strong bathymetric forcing (the Agulhas Plateau is centered at 26°E). The four intervals marked correspond to the meander being centered at 26.6°E, 25.8°E, 26.4°E, and finally 25.0°E. Modeling studies by [Lutjeharms and van Ballegooyen \(1984\)](#) indicate that changes in bottom velocity could produce slight adjustments in the path of the ARC around the Agulhas Plateau, but what is new here is that we have observed that the position usually remains fixed for six or more months at a time. This meander around the Agulhas Plateau is not present during October 2000 to March 2001, due to the AC adopting a more southerly route.

A more detailed inspection of the behavior of this loop affords two other observations. First, the occasional reestablishments of stability usually involve movement to the east (e.g., Nov 1998, Jun 1999, Jun 2000), that is, they have been preceded by an abrupt change that left the loop to the west of its stable position. The second point of interest is that within the long periods of stable loop position (e.g., Aug 1999 to Apr 2000) there are many small-scale variations in the loop position, with a timescale of ~ 20 days. These may indicate some resonance period about the stable position. This would be interesting to investigate further, however the oscillations are not much larger than the resolution of the TMI, so the use of additional datasets would be necessary.

5. Conclusions

The ability to observe SST through clouds will revolutionise the study of rapidly evolving systems ([Wentz et al. 2000](#)). We have examined the TMI data for two very active ocean systems: the Agulhas and East Madagascar Retroreflections. The region is notorious for the cloud cover impact on infrared observations; [van Leeuwen et al. \(2000\)](#) could not observe the sea surface for 50 days at a time. As the TMI SST fields are spatially complete we have been able to automate the detection and tracking of features, whereas infrared analyses through patchy cloud have needed human subjective interpretation to detect ([Lutjeharms and van Ballegooyen 1988](#)) and monitor features ([van Leeuwen et al. 2000](#)). The TMI analysis shows a number of positive anomalies moving poleward along the east coast of South Africa, with propagation characteristics similar to those of Natal pulses. Although the Agulhas retroreflection itself was outside of the TMI's coverage, we can see convincing westward progradations of the current, with about eight events per year, consistent with other estimates, during the period December 1997 to March 2000. Thereafter, we have observed a change in the behaviour of the Agulhas retroreflection, with the retroreflection occurring farther to the east. This may be due to a strengthening of the Agulhas Current, possibly associated with changes in Indian Ocean circulation (see discussion in [Quarty and Srokosz 1993](#)) and requires further investigation (beyond the scope of this paper). Many Agulhas rings appear to show up as warm or cold anomalies, drifting to the west or northwest. However, they cannot be tracked for long because of the rapid loss of surface thermal signature ([Walker and Mey 1988](#)). The new observations of the East Madagascar retroreflection are intriguing in that the majority of warm features appear to head south and then southwest, although this could be because those going west have minimal SST anomaly and cannot be detected by the methods used here.

Finally, we have made new observations of the position of the topographically controlled meander in the ARC at ~ 26°E and found that its position varies in an unexpected manner; remaining fixed for months and then shifting abruptly to the east or west by ~ 0.5° or more. There also appears to be small-scale variability in this feature on a timescale of ~ 20 days. Both of these findings warrant further investigation.

This paper has demonstrated the many different insights into the circulation in this region that can be obtained from TMI data alone, including observations of some unexpected and as yet unexplained changes in the AC and ARC. Naturally, a clearer picture would be obtained if these were combined with altimetry. This would help to decide whether the features along the Mozambique Ridge are indeed cold core cyclonic eddies with a warm cap, and also aid in the interpretation and tracking of the near-coastal features. This is the subject of future work.

Acknowledgments

We are grateful to EORC/NASDA for the provision of the TMI SST data.

REFERENCES

- Biastoch A., and W. Krauss, 1999: The role of mesoscale eddies in the source regions of the Agulhas Current. *J. Phys. Oceanogr.*, **29**, 2303–2317. [Find this article online](#)
- de Ruijter W. P. M., A. Biastoch, S. S. Drijfout, J. R. E. Lutjeharms, R. P. Matano, T. Pichevin, P. J. Van Leeuwen, and W. Weijer, 1999a: Indian–Atlantic interocean exchange: Dynamics, estimation and impact. *J. Geophys. Res.*, **104**, 20885–20910. [Find this article online](#)
- de Ruijter W. P. M., P. J. van Leeuwen, and J. R. E. Lutjeharms, 1999b: Generation and evolution of Natal Pulses: Solitary meanders in the Agulhas Current. *J. Phys. Oceanogr.*, **29**, 3043–3055. [Find this article online](#)

de Ruijter W. P. M., H. Ridderinkhof, J. R. E. Lutjeharms, M. W. Schouten, and C. Veth, 2001: Observations of the flow in the Mozambique Channel. *Geophys. Res. Lett.*, in press.

Feron R. V. C., W. P. M. de Ruijter, and D. Oksam, 1992: Ring shedding in the Agulhas Current system. *J. Geophys. Res.*, **97**, 9467–9477. [Find this article online](#)

Goni G. J., S. L. Garzoli, A. J. Roubicek, D. B. Olson, and O. B. Brown, 1997: Agulhas ring dynamics from TOPEX/POSEIDON satellite altimeter data. *J. Mar. Res.*, **55**, 861–883. [Find this article online](#)

Gründlingh M. L., 1979: Observation of a large meander in the Agulhas Current. *J. Geophys. Res.*, **84**, 3776–3778. [Find this article online](#)

Gründlingh M. L., 1983: Eddies in the Southern Indian Ocean and Agulhas Current. *Eddies in Marine Science*, A. R. Robinson, Ed., Springer-Verlag, 245–264.

Gründlingh M. L., 1985: An intense cyclonic eddy east of the Mozambique Ridge. *J. Geophys. Res.*, **90**, 7163–7167. [Find this article online](#)

Kummerow C., W. Barnes, K. Toshiaki, J. Shiue, and J. Simpson, 1998: The Tropical Rainfall Measuring Mission (TRMM) sensor package. *J. Atmos. Oceanic Technol.*, **15**, 809–817. [Find this article online](#)

Lutjeharms J. R. E., 1988a: Remote sensing corroboration of retroflexion of the East Madagascar Current. *Deep-Sea Res.*, **35**, 2045–2050. [Find this article online](#)

Lutjeharms J. R. E., 1988b: On the role of the East Madagascar Current as a source of the Agulhas Current. *S. Afr. J. Sci.*, **84**, 236–238. [Find this article online](#)

Lutjeharms J. R. E., and R. C. van Ballegooyen, 1984: Topographic control in the Agulhas Current system. *Deep-Sea Res.*, **31**, 1321–1337. [Find this article online](#)

Lutjeharms J. R. E., and H. R. Roberts, 1988: The Natal pulse: An extreme transient on the Agulhas Current. *J. Geophys. Res.*, **93**, 631–645. [Find this article online](#)

Lutjeharms J. R. E., and H. R. Valentine, 1988: Eddies at the subtropical convergence south of Africa. *J. Phys. Oceanogr.*, **18**, 761–774. [Find this article online](#)

Lutjeharms J. R. E., and R. C. van Ballegooyen, 1988: The Retroflexion of the Agulhas Current. *J. Phys. Oceanogr.*, **18**, 1570–1583. [Find this article online](#)

Lutjeharms J. R. E., O. Boebel, P. C. F. van der Vaart, W. P. M. de Ruijter, T. Rossby, and H. L. Bryden, 2001: Evidence that the Natal pulse involves the Agulhas Current to its full depth. *Geophys. Res. Lett.*, **28**, 3499–3452. [Find this article online](#)

Olson D. B., and R. H. Evans, 1986: Rings of the Agulhas Current. *Deep-Sea Res.*, **33**, 27–42. [Find this article online](#)

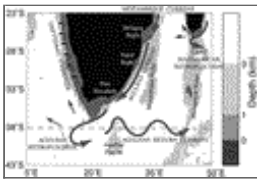
Quartly G. D., and M. A. Srokosz, 1993: Seasonal variations in the region of the Agulhas Retroflexion: Studies with Geosat and FRAM. *J. Phys. Oceanogr.*, **23**, 2108–2124. [Find this article online](#)

Schouten M. W., W. P. M. de Ruijter, P. J. van Leeuwen, and J. R. E. Lutjeharms, 2000: Translation, decay and splitting of Agulhas rings in the southeastern Atlantic Ocean. *J. Geophys. Res.*, **105**, 21913–21925. [Find this article online](#)

Van Leeuwen P. J., W. P. M. de Ruijter, and J. R. E. Lutjeharms, 2000: Natal pulses and the formation of Agulhas rings. *J. Geophys. Res.*, **105**, 6425–6436. [Find this article online](#)

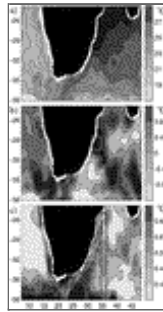
Walker N. D., and R. D. Mey, 1988: Ocean/atmosphere heat fluxes within the Agulhas Retroflexion region. *J. Geophys. Res.*, **93**, 15475–15483. [Find this article online](#)

Wentz F. J., C. Gentemann, D. Smith, and D. B. Chelton, 2000: Satellite measurements of sea surface temperature through clouds. *Science*, **288**, 847–850. [Find this article online](#)



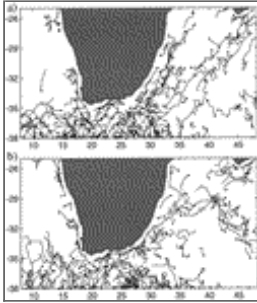
Click on thumbnail for full-sized image.

FIG. 1. Schematic of Agulhas Current System, with the key bathymetric features marked



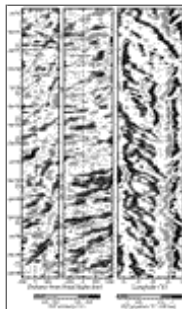
Click on thumbnail for full-sized image.

FIG. 2. (a) Smoothed SST field for 23–28 Jan 1999. (b) Same field after five EOFs removed. (c) Rms variability of SST field after the first five EOFs have been removed. (The regions with dashed borders are discussed in [section 4](#))



Click on thumbnail for full-sized image.

FIG. 3. (a) Tracks of 250 features that maintain an SST anomaly of at least 0.4°C for 20 days or more. (A dot marks the start of each track.) (b) The same for anomalies below -0.4°C



Click on thumbnail for full-sized image.

FIG. 4. (a) Hovmöller diagram of spatially averaged SST anomaly between 34.5° and 36.5°E. Dashed lines indicate seven probable events, with circled number on left axis. (The abscissa give the distance from the Natal Bight at 29.5°S.) (b) Hovmöller diagram of spatially averaged anomaly in coastal section marked on [Fig. 2c](#). Circled letters on left of axis refer to the nine highlighted events discussed in the text. The circles denote sea surface depressions observed at 29°E, 32°S along the coast. (Abscissa is distance from the Natal Bight, with Port Elizabeth, where the mean current leaves the shore, being ~ 900 km along coast.) (c) Hovmöller diagram of zonal gradient of SST at 38°S. Dashed lines emphasise possible progradations of the AR; the dotted lines indicate the position of the first cold loop of the ARC.



© 2008 American Meteorological Society [Privacy Policy and Disclaimer](#)
Headquarters: 45 Beacon Street Boston, MA 02108-3693
DC Office: 1120 G Street, NW, Suite 800 Washington DC, 20005-3826
amsinfo@ametsoc.org Phone: 617-227-2425 Fax: 617-742-8718
[Allen Press, Inc.](#) assists in the online publication of *AMS* journals.